Stretched-exponential *a*-Si:H/*c*-Si interface recombination decay

Stefaan De Wolf,[a] Sara Olibet, and Christophe Ballif
University of Neuchâtel, Breguet 2, CH-2000 Neuchâtel, Switzerland

(Received 23 May 2008; accepted 18 June 2008; published online 23 July 2008)

The electronic properties of hydrogenated amorphous silicon (*a*-Si:H) relax following stretched exponentials. This phenomenon was explained in the past by dispersive hydrogen diffusion, or by retrapping included hydrogen motion. In this letter, the authors report that the electronic passivation properties of intrinsic *a*-Si:H/crystalline silicon (*c*-Si) interfaces relax following a similar law. Carrier injection dependent *a*-Si:H/*c*-Si interface recombination calculations suggest this originates from amphoteric interface state (or Si dangling bond) reduction, rather than from a field effect. These findings underline the similarity between *a*-Si:H/*c*-Si interface recombination and the electronic properties of *a*-Si:H bulk material. © *2008 American Institute of Physics*.
[DOI: 10.1063/1.2956668]

Outstanding electronic passivation of wafer surfaces is a key element for high performance crystalline silicon (*c*-Si) solar cells.[1] This can be achieved either by an electrical field effect, repelling electrons or holes from the electronically active surface states, or by reduction of the surface state density. The latter may be accomplished by hydrogenation of silicon dangling bonds present on *c*-Si surfaces.[2] Related to this, record surface passivation has been demonstrated by immersion of *c*-Si surfaces in HF based solutions.[3] Alternatively, *c*-Si surface dangling bond passivation may also be obtained by deposition of intrinsic hydrogenated amorphous silicon (*a*-Si:H) films.[4] As such films can, in addition, be doped relatively easily, they allow for the fabrication of electronically abrupt *a*-Si:H/*c*-Si heterojunctions.[5] Since direct deposition of such doped films on *c*-Si can result in poor interface properties, typically, a few nanometer thin intrinisic *a*-Si:H(*i*) buffer layer is inserted in between for *a*-Si:H/*c*-Si heterostructure solar cell fabrication.[6] Impressive large area (>100 cm^2) energy conversion efficiencies ($>22\%$) have been reported for such devices.[7] For this, atomically sharp *a*-Si:H/*c*-Si interfaces, i.e., where no epitaxial Si (epi-Si) film was grown on the wafer during film deposition, are considered to be essential.[8] This can be monitored in real time by various optical probes.[9,10] On a related note, the excellent *a*-Si:H/*c*-Si interface passivation properties may also offer an explanation why surrounding *a*-Si:H tissue is crucial for device-grade microcrystalline Si.[11] Nevertheless, the relation between processing parameters and the physical mechanism underlying the *a*-Si:H/*c*-Si interface passivation is not yet fully understood.

Previously it was suggested that low-temperature annealing is beneficial for the interface passivation quality, provided that neither epi-Si at the interface[12] nor boron-doped overlayer[13,14] is present. In this letter, we show that under these conditions electronic passivation relaxation can be accurately described by stretched exponentials. It is observed that even moderate temperature ($\leqslant 180\,^\circ$C) annealing can yield an extremely low interface recombination activity. Carrier injection dependent recombination calculations suggest that the origin of this phenomenon is related to dangling bond reduction at the interface, rather than to a field effect. Consequently, similar to the SiO_2/*c*-Si interface,[15] also here, a strong analogy between the nature of the defects present at the *a*-Si:H(*i*)/*c*-Si interface and those in the *a*-Si:H(*i*) bulk may possibly exist.

For the experiments, 300 μm thick $\sim$3.0 Ω cm phosphorus-doped high quality float zone (100) FZ-Si wafers were used. Both substrate surfaces were mirror polished to eliminate the influence of substrate surface roughness on the passivation properties.[16] Surface cleaning simply consisted of native oxide stripping in a dilute HF solution (4%) for 45 s, after which the samples were immediately transferred to the load lock of the deposition system. For *a*-Si:H film deposition, a standard capacitively coupled parallel plate plasma enhanced chemical vapor deposition system was used. The power generator was operated in the very high frequency (70 MHz) regime. The electrode distance was 14 mm. A power density of 15 mW cm^{-2} was used. The SiH_4-flow and the process pressure, respectively, equaled 11 SCCM (SCCM denotes cubic centimeter per minute at STP), diluted in 29 SCCM H_2 and 0.3 Torr. These conditions gave a deposition rate of $\sim$3.1 Å s^{-1} for intrinsic films. For all depositions, the value for T_{depo} was varied between 130 and 180 °C. The samples were mounted at the top electrode to avoid dust incorporation in the films. Prior to all depositions the wafer surfaces were exposed to a 50 SCCM H_2 flow at 0.45 Torr for 20 min for substrate temperature stabilization. For each temperature, films with about 50 nm thickness were deposited on both wafer surfaces to evaluate the surface passivation quality. Following this, the samples were consecutively subjected to isothermal annealing treatments in air for prolonged times t_{ann}. The value for the effective carrier lifetime τ_{eff} of the samples was measured with a Sinton Consulting WCT-100 quasi-steady-state photoconductance system,[17] operated either in the so-called *generalized*,[18] or transient mode. For this, the annealing treatments were shortly interrupted. To confirm that no epi-Si was present at the interface, high resolution transmission electron microscopy (HR-TEM) images were taken of the interfaces: A sharp *a*-Si:H/*c*-Si transition was observed for films deposited at $T_{\mathrm{depo}}=200\,^\circ$C, which is shown in the inset in Fig. 1.

Figure 1 shows how the value for τ_{eff} changes over time when bifacially *a*-Si:H passivated *c*-Si wafers are subjected

[a]Electronic mail: stefaan.dewolf@unine.ch.

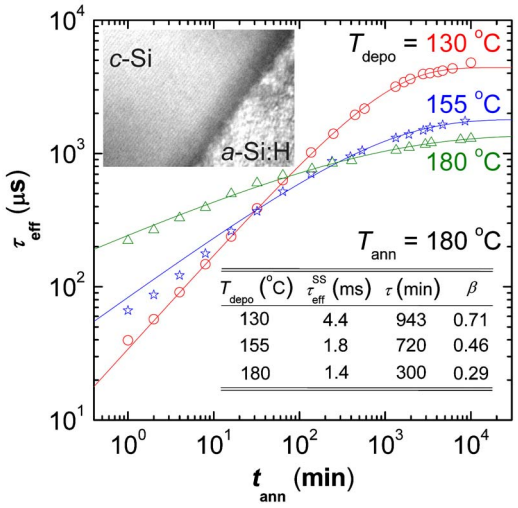

FIG. 1. (Color online) Measured values for τ_{eff} as function of t_{ann} for a ~3.0 Ω cm FZ wafer bifacially passivated by ~50 nm *a*-SiH(*i*) films. The cases for three different deposition temperatures are shown. Evaluation was performed at $\Delta n = \Delta p = 1.0 \times 10^{15}$ cm^{-3}. The annealing temperature was fixed at 180 °C. Symbols represent measured data. Solid lines represent stretched-exponential fits to the data. Values for the fitting parameters are given in the inset table. The inset HR-TEM micrograph is taken from one of the interfaces of a mirror-polished *c*-Si (100) sample featuring *a*-Si:H films for which T_{depo}=200 °C.

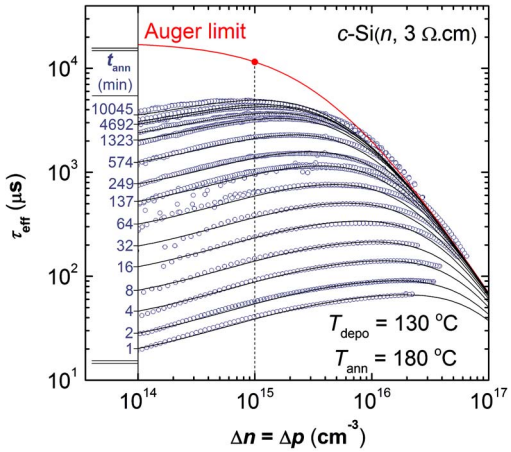

FIG. 2. (Color online) Measured values for τ_{eff} as function of the carrier injection level for films deposited at 130 °C. The different curves show data after different annealing times. The annealing temperature was fixed at 180 °C. Symbols represent measured data, whereas solid lines show calculated recombination-model fits. The uppermost curve shows the bulk-limited value for τ_{eff}.

to isothermal annealing. The lowest deposition temperatures give for as-deposited films values for τ_{eff} as poor as 12.2 μs at an injection level of 1.0×10^{15} cm^{-3}. Interestingly, the same sample yields under sufficiently long annealing a value for τ_{eff} in excess of 4 ms. Irrespective of the value for T_{depo}, the shown data can be fitted with satisfying accuracy to stretched exponentials of the form,

$$\tau_{eff}(t_{ann}) = \tau_{eff}^{SS}\left\{1 - \exp\left[-\left(\frac{t_{ann}}{\tau}\right)^{\beta}\right]\right\}, \quad (1)$$

where τ_{eff}^{SS} is the saturation value for τ_{eff}, β and τ the dispersion parameter ($0 < \beta < 1$), and effective time constant, respectively. From the figure, it is seen that in the present case different values for T_{depo} render different values for τ_{eff}^{SS}, which may have important device processing implications. Figure 2 shows, for films deposited at 130 °C, τ_{eff} curves as function of the carrier injection density. Here, these measurements have been fitted to recombination calculations at the *a*-Si:H/*c*-Si interface.[19] Briefly, these calculations form an extension of the formalism developed by Girisch *et al.* to compute recombination parameters of the SiO_2/*c*-Si interface.[20] In the present case, the assumption is made that the interface recombination is occurring through amphoteric defects.[21] In the current formalism, the two model parameters are the dangling bond surface density N_{DB}^{S} and the charge density at the interface Q_S. Electronically, the amphoteric defects (i.e., dangling bonds) are characterized by their electron and hole capture cross sections, respectively in the neutral states σ_n^0 and σ_p^0 and the charged states σ_n^+ and σ_p^-. The following relations, similar to the *a*-Si:H bulk values, were found for the interface dangling bond capture cross section ratios:[19] $\sigma_p^0/\sigma_n^0 = 20$ and $\sigma_n^+/\sigma_n^0 = \sigma_p^-/\sigma_p^0 = 500$. Figure 2 shows that the experimental data can be well fitted by the employed calculations. The uppermost solid curve represents the maximum bulk lifetime based on the Auger recombination parameterization by Kerr and Cuevas.[22] Similarly, numerical fitting, but based on device simulation software, was recently used to study the presumed light-induced defect generation at a 10 nm thin *a*-Si:H(*i*)/*c*-Si interface.[23] Interestingly, the only parameter that needs to be changed to yield a good fit in Fig. 2 is in all cases N_{DB}^{S}. The value for Q_S can be kept constant at -2.2×10^{10} cm^{-2}. Physically, the fact that Q_S does not change by annealing implies that the outstanding passivation obtained by such a treatment is not caused by a field effect and suggests it is in fact N_{DB}^{S} that decays following stretched exponentials. The latter point is confirmed in Fig. 3. Here, panel (a) shows the relation between the calculated N_{DB}^{S} values and the experimental value of τ_{eff} (at $\Delta n = 1.0 \times 10^{15}$ cm^{-3}). Only for $\tau_{eff} > \sim 2$ ms, a deviation of the data from a $\tau_{eff}^{-1} \sim N_{DB}^{S}$ law can be seen, indicating that bulk-recombination processes start to limit here the value for τ_{eff}. Note that the asymptote is not equal to the *c*-Si Auger limit, suggesting that other bulk-recombination mechanisms may

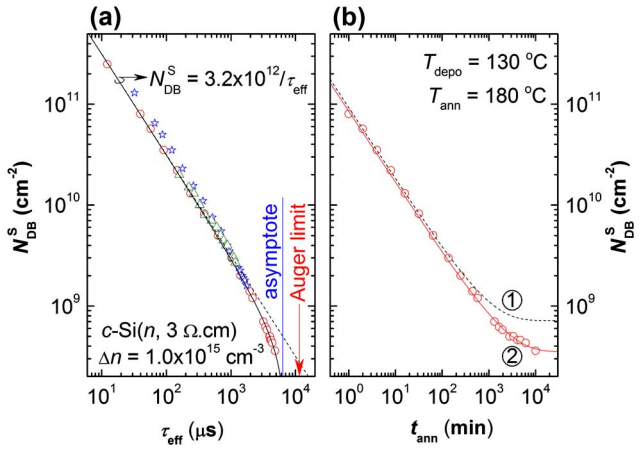

FIG. 3. (Color online) (a) Calculated values for N_{DB}^{S} vs the experimental value of τ_{eff}, evaluated at $\Delta n = 1.0 \times 10^{15}$ cm^{-3}. For all fits, $Q_S = -2.2 \times 10^{10}$ cm^{-2}. The different symbols correspond with those of the experimental data shown in Fig. 1. Dashed line shows a $\tau_{eff}^{-1} \sim N_{DB}^{S}$ law. Solid line is a guide for the eye. (b) Calculated values for N_{DB}^{S} vs t_{ann}. Symbols represent data extracted from the fits in Fig. 2. Solid line represents calculated stretched-exponential fit. Dashed line represents the fit, as shown in Fig. 1. to the T_{depo}=130 °C data, converted by the $N_{DB}^{S} \sim \tau_{eff}^{-1}$ law.

limit the carrier lifetime in the *c*-Si bulk. Panel (b) in the same figure shows calculated values for N_{DB}^{S} versus t_{ann}. Symbols represent data extracted from the fits in Fig. 2. The dashed line (label 1) represents the same fit as shown in Fig. 1 to the $T_{depo}=130\ ^{\circ}C$ data, converted by the $\tau_{eff}^{-1}\sim N_{DB}^{S}$ law. Evidently, this curve follows the same stretched-exponential functional, as described in Fig. 1 for the $T_{ann}=130\ ^{\circ}C$ data. The solid line (label 2) represents a newly calculated fit to the N_{DB}^{S} data now to a functional which is inverse proportional to relation (1). Here the effect of a finite bulk lifetime was taken into account. A good fit can be obtained in this case, suggesting that it is indeed likely to be the surface dangling bond density that decays following stretched exponentials.

Stretched-exponential decay[24] is a characteristic phenomenon that often describes the relaxation of disordered systems toward equilibrium. For bulk *a*-Si:H, relaxation is governed by release of hydrogen from trap sites.[25] Dispersive diffusion of hydrogen, arising from a distribution of energies for trap states and barrier heights, has been argued to yield the observed stretched-exponential relaxation.[25] An alternative explanation was given by Van de Walle, considering the fact that hydrogen in transition between a source *trap* state and a (lower energy) sink *reservoir* state can be retrapped at the same or at another trap site.[26,27] The latter considerations yield a functional form behaving much like the traditional stretched exponential.[26] In practice, the hydrogen reservoir could be assumed to exist in a monohydride form,[26] whereas for the trapped hydrogen perhaps this is in the form of a higher hydride configuration. For the *a*-Si:H/*c*-Si heterostructure, for as-deposited material close to the interface, the hydride modes at higher (lower) stretching frequencies are more (less) dominant than several nanometer into the *a*-Si:H film.[28] This suggests the presence of a sufficient amount of trapped hydrogen close to the interface of which a fraction may be easily excited to a mobile state. In addition to this, infrared transmission measurements on very thin *a*-Si:H films at the Brewster angle have suggested that annealing of *a*-Si:H/*c*-Si structures yields a transfer of hydrogen to a monohydride *c*-Si surface (reservoir) state.[29] Finally, lowering the value for T_{depo} typically yields an increasing $Si-H_{n>1}/Si-H$ ratio. This fact may offer an explanation why, provided the annealing time is sufficiently long, the films deposited at the lowest temperatures, as given in Fig. 1, result in the lowest recombination activity, and why in case epi-Si is present, which likely contains only miniscule amounts of higher hydrides, the interface passivation degrades under annealing.[12]

To summarize, the shown annealing induced passivation improvement suggests that a low *a*-Si:H/*c*-Si interface recombination activity and device-grade bulk *a*-Si:H are largely governed by very similar defects, i.e., their Si dangling bond densities at the interface and in the bulk. In addition, the observed stretched-exponential-like behavior may offer insight in the role that hydrogen plays in the interface passivation kinetics.

This work was supported by the European Community's Seventh Framework Programme [FP7/2007-2013] under the Hetsi Project (Grant Agreement No. 211821), and Axpo Holding AG, Switzerland in the frame of the Axpo Naturstrom Fond. Evelyne Vallat-Sauvain is thanked for kindly providing the HR-TEM micrograph.

[1] A. G. Aberle, in *Crystalline Silicon Solar Cells: Advanced Surface Passivation and Analysis* (University of New South Wales, Sydney, 1999).
[2] J. I. Pankove, M. A. Lampert, and M. L. Tarng, Appl. Phys. Lett. **32**, 439 (1978).
[3] E. Yablonovitch, D. L. Allara, C. C. Chang, T. Gmitter, and T. B. Bright, Phys. Rev. Lett. **57**, 249 (1986).
[4] J. I. Pankove and M. L. Tarng, Appl. Phys. Lett. **34**, 156 (1979).
[5] H. Matsuura, T. Okuno, H. Okushi, and K. Tanaka, J. Appl. Phys. **55**, 1012 (1984).
[6] M. Tanaka, M. Taguchi, T. Matsuyama, T. Sawada, S. Tsuda, S. Nakano, H. Hanafusa, and Y. Kuwano, Jpn. J. Appl. Phys., Part 1 **31**, 3518 (1992).
[7] Y. Tsunomura, Y. Yoshimine, M. Taguchi, T. Kinoshita, H. Kanno, H. Sakata, E. Maruyama, and M. Tanaka, Technical Digest of the 17th International Photovoltaic Science and Engineering Conference, Fukuoka, Japan, 2007 (unpublished), p. 387.
[8] T. H. Wang, E. Iwaniczko, M. R. Page, D. H. Levi, Y. Yan, H. M. Branz, and Q. Wang, Thin Solid Films **501**, 284 (2006).
[9] H. Fujiwara and M. Kondo, Appl. Phys. Lett. **90**, 013503 (2007).
[10] J. J. H. Gielis, P. J. van den Oever, M. C. M. van de Sanden, and W. M. M. Kessels, Appl. Phys. Lett. **90**, 202108 (2007).
[11] J. Meier, R. Flückiger, H. Keppner, and A. Shah, Appl. Phys. Lett. **65**, 860 (1994).
[12] S. De Wolf and M. Kondo, Appl. Phys. Lett. **90**, 042111 (2007).
[13] S. De Wolf and G. Beaucarne, Appl. Phys. Lett. **88**, 022104 (2006).
[14] S. De Wolf and M. Kondo, Appl. Phys. Lett. **91**, 112109 (2007).
[15] D. K. Biegelsen, N. M. Johnson, M. Stutzmann, E. H. Poindexter, and P. J. Caplan, Appl. Surf. Sci. **22/23**, 879 (1985).
[16] S. De Wolf, G. Agostinelli, G. Beaucarne, and P. Vitanov, J. Appl. Phys. **97**, 063303 (2005).
[17] R. A. Sinton and A. Cuevas, Appl. Phys. Lett. **69**, 2510 (1996).
[18] H. Nagel, C. Berge, and A. G. Aberle, J. Appl. Phys. **86**, 6218 (1999).
[19] S. Olibet, E. Vallat-Sauvain, and C. Ballif, Phys. Rev. B **76**, 035326 (2007).
[20] R. B. M. Girisch, R. P. Mertens, and R. F. de Keersmaecker, IEEE Trans. Electron Devices **35**, 203 (1988).
[21] F. Vaillant and D. Jousse, Phys. Rev. B **34**, 4088 (1986).
[22] M. J. Kerr and A. Cuevas, J. Appl. Phys. **91**, 2473 (2002).
[23] H. Plagwitz, B. Terheiden, and R. Brendel, J. Appl. Phys. **103**, 094506 (2008).
[24] R. Kohlrausch, Ann. Phys. **12**, 393 (1847).
[25] J. Kakalios, R. A. Street, and W. B. Jackson, Phys. Rev. Lett. **59**, 1037 (1987).
[26] C. G. Van de Walle, Phys. Rev. B **53**, 11292 (1996).
[27] We follow here the terminology (trap and reservoir) as in Ref. 26.
[28] H. Fujiwara and M. Kondo, Appl. Phys. Lett. **86**, 032112 (2005).
[29] M. Z. Burrows, U. K. Das, R. L. Opila, S. De Wolf, and R. W. Birkmire, J. Vac. Sci. Technol. A **26**, 683 (2008).